CURIOSIS

APPLICATION NOTE

Real-Time Imaging and Automated Quantification of Wound Closure Dynamics with Celloger® Pro

■ Introduction

Cell migration is a fundamental biological process involved in wound healing, tissue regeneration, and cancer metastasis.[1] The wound healing assay, also known as the scratch assay, is widely used *in vitro* method to evaluate migratory capacity by monitoring how cells move to close an artificially created gap under different stimuli.

Accurately distinguishing differences in migration patterns across conditions is essential for understanding the regulatory mechanisms of cell movement and for evaluating the effects of potential therapeutic agents. For example, changes in growth factor availability (e.g., serum concentration) and drug-induced cytoskeletal modulation can significantly influence wound closure dynamics, making robust quantification essential to avoid misinterpretation of experimental outcomes. However, conventional approaches that rely on manual imaging and analysis can be time-consuming and often lack reproducibility, particularly when multiple conditions or subtle phenotype differences must be compared. Automated time-lapse imaging with standardized acquisition and analysis can help overcome these limitations by reducing user-dependent variability and enabling more reliable comparisons.

In this application note, the Celloger® Pro automated live-cell imaging system was used to perform wound healing assays in real time under different experimental conditions, including varying fetal bovine serum (FBS) concentrations and treatment with migration-modulating drugs. The assays were quantified using Celloger®'s latest image-based analysis algorithm to enable consistent, objective measurement of wound closure dynamics across conditions. Overall, this workflow demonstrates how automated time-lapse imaging combined with quantitative image-based analysis can simplify and accelerate migration assays while providing consistent results.

■ Materials and Methods

NIH-3T3 fibroblasts were cultured in Dulbecco's Modified Eagle Medium (DMEM) supplemented with 10% FBS and 1% penicillin-streptomycin at 37°C. When cells reached approximately 90% confluence, a uniform linear scratch (wound) was generated at the center of each well using a sterile pipette tip. Immediately after scratching, wells were gently washed twice with phosphate-buffered saline (PBS) to remove detached cells and debris. Subsequently, cells were incubated in fresh DMEM supplemented with FBS at 0%, 5%, or 10%. For drug treatment experiments, cells were maintained in DMEM containing 10% FBS and treated with staurosporine (10 nM), cytochalasin B (1.2 μM), and doxorubicin (50 nM). Time-lapse imaging was performed every 30 minutes for 72 hours. Wound area was quantified from bright-field (BF) images using the Celloger Analysis App.

■ Results

Wound closure rate was used as an indicator of cellular motility and recovery capacity under different experimental conditions. The Celloger Analysis App provides multiple modes tailored to different cellular structures and experimental purposes. In **Wound Area** mode, the software distinguishes the scratched region from cell-covered areas and displays the detected wound area as a yellow overlay (Figure 1). Wound area was measured at each time point using a high-accuracy analysis algorithm, and wound closure rate (%) was calculated as follows:

$$Wound\ Closure\ \% = \left[\frac{A_{t=0h} - A_{t=\Delta h}}{A_{t=0h}}\right] \times 100\ \%$$

* $A_{t=0h}$ is the area of the wound measured immediately after scratching. (t=0h)
* $A_{t=\Delta h}$ is the area of the wound measured *h* hours after the scratch is performed.

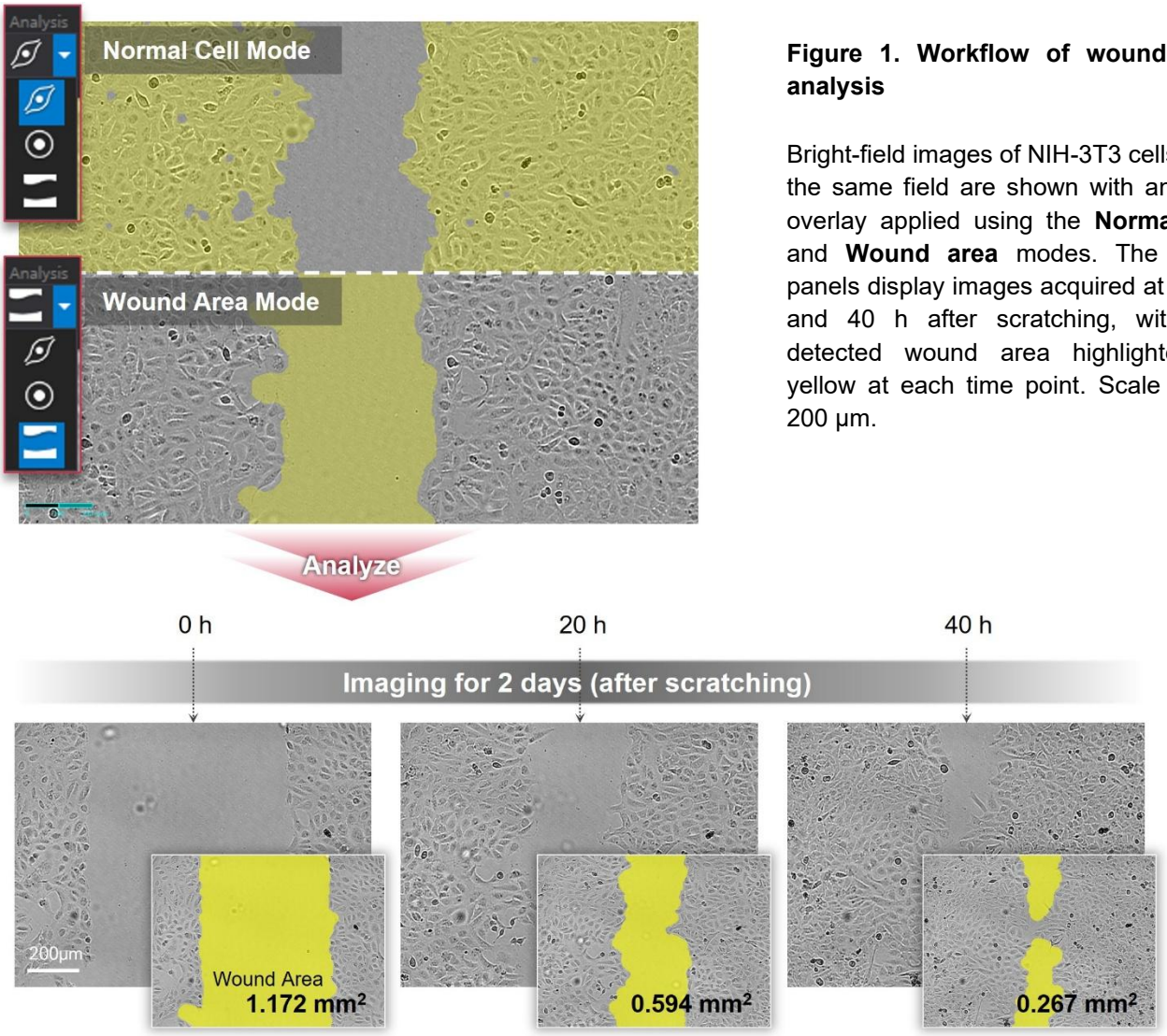

Figure 1. Workflow of wound area analysis

Bright-field images of NIH-3T3 cells from the same field are shown with analysis overlay applied using the **Normal cell** and **Wound area** modes. The lower panels display images acquired at 0, 20, and 40 h after scratching, with the detected wound area highlighted in yellow at each time point. Scale bar = 200 μm.

To begin with, temporal changes in wound closure (%) under different FBS concentrations (0%, 5%, and 10%) were compared (Figure 2). With identical initial wound areas, wound closure was delayed in the 0% FBS condition, indicating reduced recovery capacity. In contrast, wound closure progressed rapidly in the 10% FBS condition, consistent with enhanced cell migration and proliferation (Figure 2A). The 5% FBS condition also showed closure, but at a slower rate than the 10% FBS condition. Quantitative analysis confirmed that the 10% FBS condition exhibited the steepest increase over time, whereas the 0% FBS condition showed only a slight change, highlighting that growth factor content in the medium significantly affects cell motility and wound closure dynamics (Figure 2B).

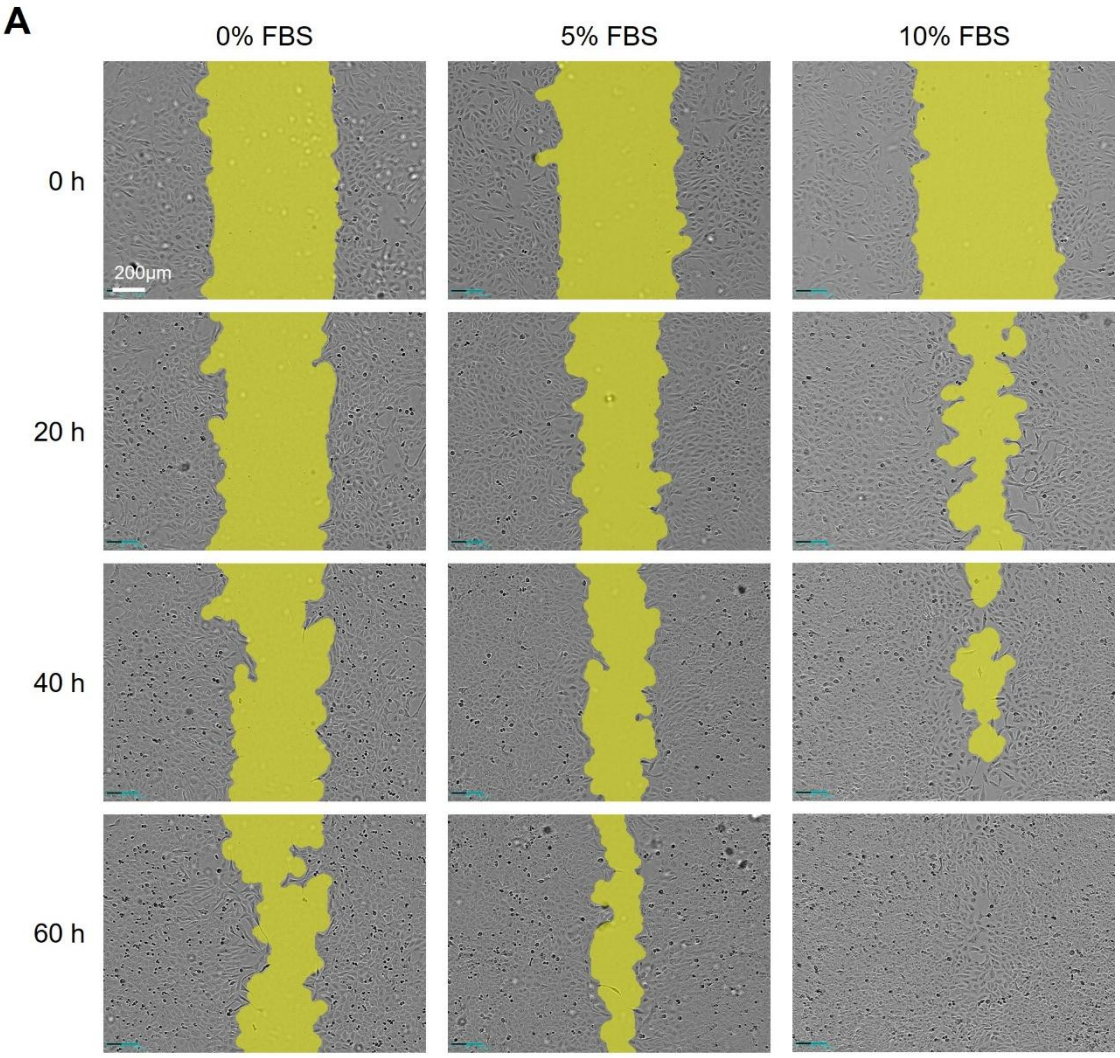

Figure 2. Effect of FBS concentration on wound closure

(**A**) Representative bright-field images of wound-healing assays under 0%, 5%, and 10% FBS conditions at 0, 20, 40, and 60 h after scratching. The wound area is highlighted in yellow. Scale bars = 200 μm. (**B**) Quantitative wound closure curves over 72 hours. Cells cultured in 10% FBS exhibited the fastest closure, followed by 5% FBS, while closure in 0% FBS was delayed.

In addition to serum conditions, wound closure can be influenced by cell migration, proliferation, and cell death. To examine how perturbing these processes alters closure kinetics, additional wound-healing assays were performed with staurosporine, cytochalasin B, and doxorubicin at sublethal concentrations.

In representative images (Figure 3A), the 10% FBS control condition showed robust wound closure. In contrast, staurosporine, a potent apoptosis inducer[2], markedly reduced wound-healing activity. Cells displayed progressive morphological changes, including shrinkage, consistent with apoptosis (Figure 3A-B). Cell death became evident around 20 hours, causing the wound closure curve to plateau, with little to no further closure observed thereafter (Figure 3C).

Cytochalasin B also markedly reduced wound closure. Because cytochalasin B disrupts actin polymerization and impairs the cytoskeletal dynamics required for motility[3], this effect is consistent with reduced migratory capacity. No evident cell death was observed, but proliferation appeared suppressed (Figure 3B), limiting advancement of the leading edge and slowing closure (Figure 3C).

Interestingly, doxorubicin produced a wound closure rate similar to the control. As a chemotherapeutic agent that induces DNA damage[4], doxorubicin did not cause pronounced cell death under the conditions tested but appeared to suppress cell proliferation. Despite this growth inhibition, wound closure remained comparable to the control because cells showed extensive spreading while maintaining migratory activity. This suggests that suppressing proliferation alone may not be sufficient to reduce wound closure and that effective inhibition requires direct impairment of migration. Notably, under mild cytotoxic stress, doxorubicin may promote a compensatory response in which cells increase their footprint and continue collective migration despite reduced growth[5]. These results demonstrate that wound closure curves vary markedly depending on the drug applied and can be categorized into distinct patterns (e.g., steep upward, gradual upward, or flat) based on their trends.

Taken together, these findings highlight the value of live-cell imaging for interpreting wound closure dynamics, as migration- and proliferation-associated behaviors can contribute differently depending on the condition or treatment. Distinguishing the relative contributions of these processes enables more accurate assessment of wound-healing activity and provides clearer insight into how external stimuli modulate collective cell behavior.

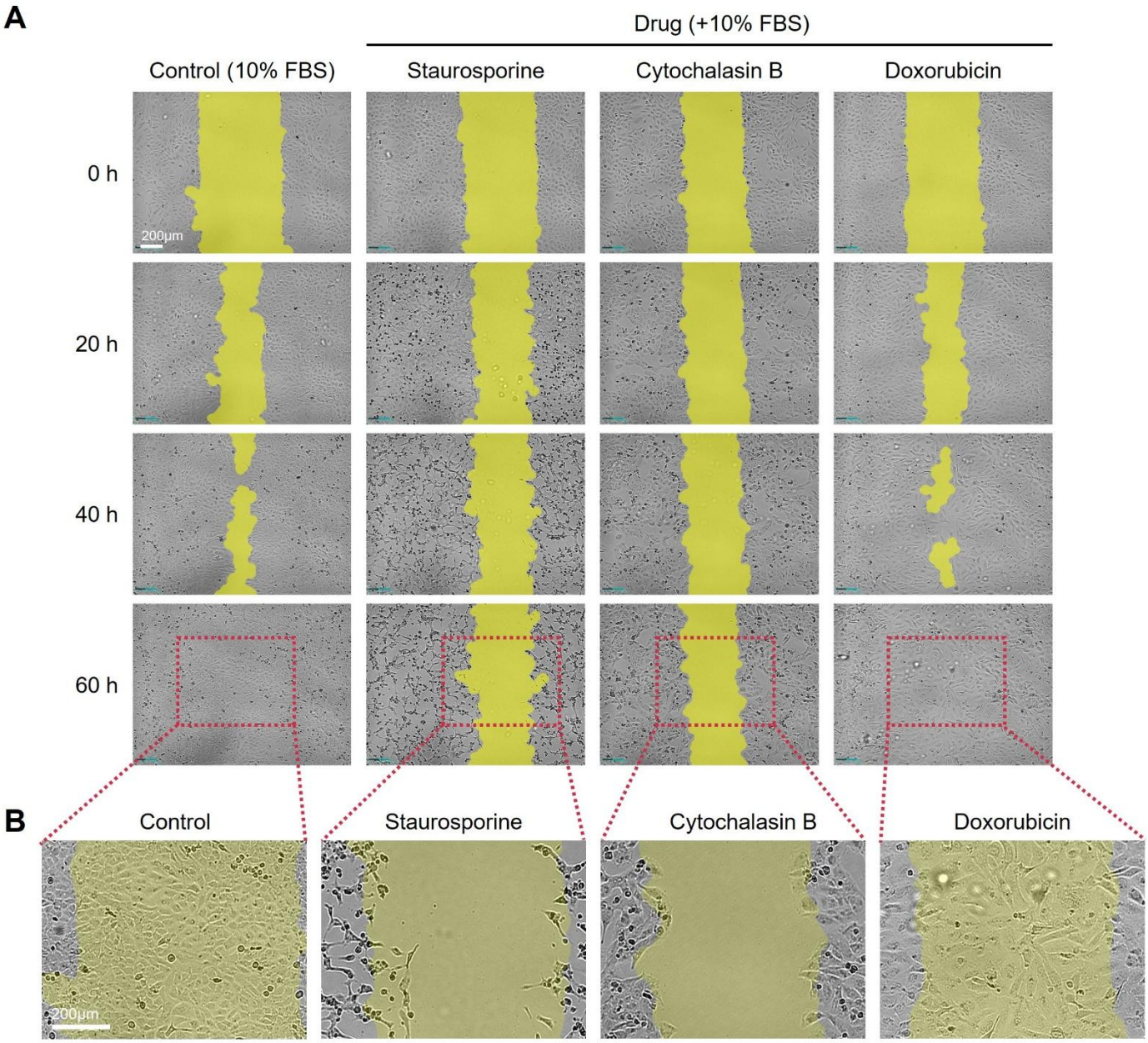

Figure 3. Effect of drug treatment on wound closure

(**A**) Representative bright-field images of wound-healing assays under 10% FBS (control) and drug-treated conditions (staurosporine, 10 nM; cytochalasin B, 1.2 µM; doxorubicin, 50 nM) at 0, 20, 40, and 60 h after scratching. The segmented wound area is highlighted in yellow. Scale bars = 200 µm. (**B**) Higher magnification views of the wound edges at 60 h for each condition. The wound area at 0 h is shown as a translucent yellow overlay for reference. (**C**) Quantification of wound closure over 72 hours for each condition.

Conclusion

This application note highlights the effectiveness of the Celloger® Pro system for wound-healing assays. Using NIH-3T3 cells, the system clearly detected differences in wound closure rates across FBS concentrations and enabled classification of distinct drug-induced closure patterns. By automating both image acquisition and wound area quantification, the system enables high-resolution, time-dependent monitoring of wound closure with minimal manual intervention.

Notably, the advanced wound detection algorithm provides accurate and consistent segmentation of the wound region, even in low-contrast or partially closed gaps. This improvement enhances the reliability of quantitative analysis and reduces user-dependent variability. Overall, the ability to clearly distinguish wound closure responses under different conditions underscores the value of Celloger® Pro as a powerful all-in-one solution for regenerative medicine research and cell motility studies.

References

1. Andries D., “A microfluidic wound-healing assay for quantifying endothelial cell migration” American Journal of Physiology (2010).
2. Chafké Ahmed Belmokhtar., “Staurosporine induces apoptosis through both caspase-dependent and caspase-independent mechanisms” Oncogene 20(3354-3362) (2001).
3. Susan MacLean-Fletcher., “Mechanism of action of cytochalasin B on actin” Cell volume 20(2) (1980).
4. Hilal Taymaz-Nikerel., “Doxorubicin induces an extensive transcriptional and metabolic rewiring in yeast cells” Scientific Reports 8(13672) (2018).
5. Samia Mohammed., “Sublethal doxorubicin promotes migration and invasion of breast cancer cells: role of Src Family non-receptor tyrosine kinases” Breast Cancer Research 23(76) (2021).